

## Diagnostic Accuracy of Magnetic Resonance Imaging Tissue Mapping in Acute Myocardial Infarction

AHMED A.M. SALAMA, M.D.\*; WALID M. KAMEL, M.D.\*\*; MAHMOUD SHAABAN, M.D.\*\*\*;  
SOHA ROMEIH, M.D.\*\*\*; AHMED KHARABISH, M.D.\*\*\*\*; AHMED RAMADAN, M.D.\*;  
MOHAMMED HOSNY, M.D.\*\*\*; REHAB M. ELNAGAR, M.D.\*\*\*; NOHA BEHAIRY, M.D.\* and  
WESAM ELMOZY, M.D.\*\*\*

*The Departments of Radiodiagnosis\*, Critical Care Medicine\*\*, Faculty of Medicine, Cairo University, Radiology Department\*\*\*, Faculty of Medicine, Tanta University, Aswan Heart Center and Radiology Department\*\*\*\*, Faculty of Medicine, Cairo University, Liverpool Heart and Chest Hospital, Liverpool, UK*

### Abstract

**Background:** Coronary artery disease (CAD) is the most common cause of death worldwide. Diagnosis of acute coronary syndrome (ACS) usually depends on the presenting symptoms, electrocardiographic findings, and serum level of cardiac enzymes. Cardiac magnetic resonance (CMR) can be helpful in suspected cases, with negative cardiac biomarkers and normal or indeterminate electrocardiographic findings. While late gadolinium enhancement (LGE) imaging is the current gold 'in vivo' standard to detect infarcted myocardial segments, the use of intravenous contrast can be problematic in patients with impaired renal function.

**Aim of Study:** We aimed to explore the diagnostic accuracy of T1 and T2 mapping to detect acutely infarcted myocardial segments, using LGE images as the 'gold standard'.

**Patients and Methods:** We retrospectively analyzed CMR scans of 40 patients presenting with acute myocardial infarction acquired within 48 hours after undergoing primary percutaneous coronary intervention. Tissue mapping values [native T1, extracellular volume (ECV), and T2] were compared between acutely infarcted and remote regions and segments, using LGE as the gold standard. ROC curve analysis was used to determine optimal cut-off values to differentiate between acutely infarcted and remote segments.

**Results:** All tissue mapping values were significantly higher in hyperenhanced (acutely infarcted) versus remote regions/segments ( $p < 0.001$  for all). Our suggested optimal cut-off values for native T1 (1095 ms) and T2 (54 ms) to differentiate hyperenhanced segments versus remote ones showed reasonable specificities (77% and 72%) and NPVs (79% for each); however, sensitivities were generally low (55% and 63%). Applying the same cut-off values to segments with no microvascular obstruction (MVO) yielded better diagnostic accuracy compared to those with MVO.

**Conclusion:** Native (non-contrast) tissue mapping has the potential to detect acutely infarcted myocardial segments with implications for the diagnostic pathways in patients with

chronic kidney disease. However, the pseudo normalization effect of MVO lowers the diagnostic accuracy of this modality, with the need to improve currently used imaging sequences to permit their routine application in clinical practice.

### List of Abbreviations:

ACS	: Acute coronary syndrome.
AUC	: Area under the curve.
CAD	: Coronary artery disease.
CBC	: Complete blood count.
CCS	: Chronic coronary syndrome.
CKD	: Chronic kidney disease.
CMR	: Cardiac magnetic resonance.
ECG	: Electrocardiogram.
ECV	: Extracellular volume.
EDV	: End diastolic volume.
EF	: Ejection fraction.
ESC	: European Society of Cardiology.
ESV	: End systolic volume.
GFR	: Glomerular filtration rate.
HE	: Hyperenhanced.
LAD	: Left anterior descending.
LCX	: Left circumflex.
LGE	: Late gadolinium enhancement.
LV	: Left ventricle.
LVOT	: Left ventricular outflow tract.
MACE	: Major adverse cardiac events.
MI	: Myocardial infarction.
MOLLI	: Modified look locker.
ms	: Millisecond.
MVO	: Microvascular obstruction.
Myo	: Myocardium.
NPV	: Negative predictive value.
NSTEMI	: ST-segment elevation myocardial infarction.
PCI	: Percutaneous coronary intervention.
PPV	: Positive predictive value.
RCA	: Right coronary artery.
ROC	: Receiver operating characteristic.
ROI	: Region of interest.
SAX	: Short axis.
SSFP	: Steady state free precession.
STEMI	: ST-segment elevation myocardial infarction.
SV	: Stroke volume.
TE	: Time to echo.
TR	: Repetition time.
TSE	: Turbo spin-echo.

**Correspondence to:** Dr. Wesam Elmozy,  
[E-Mail: wesozy@gmail.com](mailto:Wesozy@gmail.com)

**Key Words:** Acute coronary syndrome (ACS) – Coronary artery disease (CAD) – Tissue mapping – Extracellular volume (ECV) – T1 map – T2 map – Cardiac MRI.

## Introduction

**CORONARY** artery disease (CAD) is the most common cause of death worldwide [1] and is categorized into acute coronary syndromes (ACS) and chronic coronary syndromes (CCS) [2]. Diagnosis of ACS usually depends on the presenting symptoms, electrocardiographic findings, and serum level of cardiac enzymes [3]. According to the European Society of Cardiology guidelines, cardiac magnetic resonance imaging (CMR) can be used in suspected cases, with negative cardiac biomarkers and normal or indeterminate electrocardiographic findings [4].

Late gadolinium enhancement (LGE) imaging by CMR is the current gold 'in vivo' standard to identify infarcted myocardial segments [5]. However, the use of contrast agents is problematic in patients with chronic kidney disease (CKD) for fear of nephrogenic systemic fibrosis [6]. Such patients constitute up to 31% and 43% of ST elevation (STEMI) and non-ST elevation MI (NSTEMI), respectively [7]. Moreover, high-sensitivity cardiac troponin (hs-cTn) is frequently elevated at baseline in these patients [8], making the diagnosis of MI challenging, especially in absence of ST elevation. Hence, an accurate, non-contrast based CMR diagnostic modality would be particularly valuable in this patient population.

CMR tissue mapping uniquely allows quantification of proton relaxation times of the tissues helping in tissue characterization [9]. Myocardial T2 mapping is a quantitative imaging technique used for assessment of myocardial edema [10].

Native (non-contrast) CMR tissue mapping is an attractive alternative to LGE imaging for diagnosis of acute MI, obviating the need for contrast agents and potentially shortening the scan time. Several studies have confirmed significant differences in native tissue mapping values between acutely infarcted versus remote (non-infarcted) segments [11-15]. However, only few studies reported optimal cut-off values and diagnostic accuracy, mostly T1-based [13-15]. The majority were animal studies [14,15] where scanning is done under optimal conditions in anaesthetized animals, producing excellent imaging quality that cannot be guaranteed in human patients.

In this study, we aimed to explore the diagnostic accuracy of native T1 and T2 mapping to detect

acutely infarcted myocardial segments in patients presenting with acute MI within 48 hours of undergoing primary percutaneous coronary intervention (PCI), using LGE images as the 'gold standard'.

## Patients and Methods

### Study cohort:

This retrospective study involved 40 patients who presented with acute MI and underwent primary PCI between December 2015 and April 2017. The studies were performed at Aswan Heart Center. was performed within 48 hours after primary PCI. Acute MI was diagnosed based on clinical features, ECG, and cardiac biomarkers according to the fourth universal definition of MI [16]. Patients were excluded if they had a contraindication to CMR (e.g., cochlear implants or cardiac pacemaker), impaired renal function ( $GFR < 30 \text{ ml/min/1.73m}^2$ ), or if they were clinically unstable.

### Clinical and angiographic data:

Demographics and cardiovascular risk factors, including systemic hypertension, diabetes mellitus, dyslipidemia, cigarette smoking, and family history of CAD, were extracted from the medical records. Laboratory findings, including renal functions, lipid profile, and peak troponin peak level, were recorded. Finally, we collected pain duration, defined as time from the beginning of chest pain to stent insertion, and the culprit (infarct-related) artery on coronary angiography.

### CMR Imaging protocol:

CMR examination was performed using 1.5-T scanner (Avanto, Siemens Medical Systems, Erlangen, Germany) with a master gradient system (45mT/m peak gradient amplitude, 200mT/s slew rate), an 18-element array body surface coil, and 32-element spine coil. Patients were examined in the supine position, head-first, with ECG pads placed on the anterior chest wall.

### All patients underwent a standardized imaging protocol including the following sequences:

Cine steady-state free precession (SSFP) images in 4-chamber, 2-chamber, 3-chamber, and short axis (SAX) planes. Images were acquired using retrospective gating. SAX cine images were acquired as a stack from the mitral valve plane through the apex covering the entire ventricles.

**T1 mapping:** Three SAX slices (basal, mid-ventricular, and apical) were acquired using a modified Look-Locker Inversion recovery (MOLLI) sequence acquired pre-contrast and 10 minutes

post contrast administration. All images were acquired during the same cardiac phase at late diastole using the same imaging parameters with variable inversion preparation time. Typical acquisition parameters were: echo time (TE)/repetition time (TR)=1.03/413.57ms, flip angle=35°, interpolated pixel size=1.8x1.8, GRAPPA=2, and number of reference lines=24. Shimming and center frequency adjustments were performed as necessary to generate images free from off-resonance artifacts.

**T2 mapping:** Images were acquired pre-contrast in the same SAX slice positions as T1 mapping, using a gradient based sequence. All images were acquired during the same cardiac phase at late diastole using the same imaging parameters. Typical acquisition parameters were: TE/TR=52/800ms, flip angle=180°, and interpolated pixel size=2x2.

**LGE:** Delayed enhancement images for detection of hyper-enhancement, denoting MI, were obtained 6-10 minutes after IV injection of 0.15 mmol/Kg body weight gadolinium contrast agent, using an inversion recovery prepared fast gradient echo sequence. SAX LGE images were performed covering the whole ventricle, as well as 2-, 3-, and 4-chamber images, in the same slice locations as cine images. Typical scan parameters were as follows: TE/TR=3.1/6.5ms, matrix size=256 x 192, slice thickness=8mm, flip angle=20°, and bandwidth=31.2 kHz.

#### *CMR Image analysis:*

CMR images were transferred to a commercial off-line workstation (Philips Intellispace Portal version 8.0) for analysis.

#### *Evaluation of LV function:*

LV SAX endocardial borders were manually contoured at end-diastole and end-systole to determine end-diastolic (EDV) and end-systolic volumes (ESV), stroke volume (SV), and ejection fraction (EF), according to standard operational procedures adherent to the Society of Cardiovascular Magnetic Resonance (SCMR) recommendations [17]. Ventricular volumes were indexed to body surface area (BSA) calculated by Mosteller formula.

#### *Disease characterization:*

LGE images were visually assessed to identify the hyperenhanced (i.e., infarcted) segments and those with microvascular obstruction (MVO). MVO was defined as reperfusion injury despite prompt percutaneous coronary intervention after acute MI secondary to failure of restoration of myocardial blood flow at the microvascular level. MVO appears as a dark central core surrounded

by a hyperintense myocardial infarctin LGE images [18]. Hyperenhanced, thinned out myocardial segments at baseline were excluded from analysis on the assumption they developed an old MI.

Remote segments were defined as the rest of myocardial segments other than the hyperenhanced ones.

#### *T1 and T2 mapping analysis:*

The endocardial and epicardial borders were manually contoured in the pre- and post-contrast T1 and pre-contrast T2 images. Contours were drawn carefully to avoid contamination and potential partial volume effects at the endocardial and epicardial borders. Thereafter, T1 (native and post-contrast) and T2 values were automatically generated for the 16 segments (excluding the true apex) of the AHA 17-segment model [19] (Figs. 1,2), outputted on a Bull's eye diagram, using the RV insertion points as a reference. For calculation of extracellular volume (ECV), a region of interest (ROI) was drawn in the blood pool in pre- and post-contrast T1 images, and the following equation was used:

$$ECV = (1 - \text{hematocrit}) \left[ \frac{1}{T1 \text{ myo post}} - \frac{1}{T1 \text{ myo pre}} \right] / \left[ \frac{1}{T1 \text{ blood post}} - \frac{1}{T1 \text{ blood pre}} \right] \quad [20].$$

Where T1 myo is the myocardial T1 value, T1 blood is the blood T1 value, pre denotes pre-contrast and post denotes post-contrast. Individual myocardial segments with image artefacts or that were too thin were excluded from the analysis.

#### *Statistical analysis:*

Data were analyzed using R statistical package version 4.0.4 and SPSS version 27, with two-tailed  $p$ -value <0.05 indicating statistical significance. Quantitative variables were tested for normality using histograms, quantile plots, and Shapiro-Wilk tests. Normally distributed quantitative variables were expressed as mean  $\pm$  standard deviation (SD); skewed variables as median (Q1, Q3). Qualitative variables were presented as counts and percentages.

Patients with MVO versus those with no MVO were compared using independent sample  $t$ -test or its non-parametric alternative, Wilcoxon rank sum test, for quantitative variables, or Chi-square test or Fisher's test for qualitative variables.

On a per patient level, we calculated the mean tissue mapping values (native T1, ECV, and T2 values) for hyperenhanced (with acute MI) and remote regions as the average for the corresponding

segments and compared both using paired sample *t*-test or its non-parametric alternative, Wilcoxon signed-rank test.

On a segmental level, we compared tissue mapping values between hyperenhanced segments, with or without MVO, and remote segments in the entire cohort (total of 640 possible segments for the 40 patients) using one-way Welch ANOVA or Kruskal-Wallis test, with post-hoc pair-wise comparisons performed using Games-Howell test for the former and Dunn's procedure with Bonferroni correction for the latter. ROC curves were constructed to predict hyperenhancement (i.e., differentiate hyperenhanced from remote segments) from tissue mapping values, using LGE hyperenhancement as the gold standard. We used R package "cutpoint" to determine the optimal cut-off for each of the tissue mapping values based on maximizing Youden's index, defined as the sum of sensitivity and specificity minus one [21]. Bootstrapping was used to determine the 95% confidence intervals for ROC area under the curve (AUC).

## Results

### *Clinical characteristics of study cohort:*

This retrospective study involved 40 consecutive patients presenting with acute MI who subsequently underwent primary PCI: 29 males with a mean age of 53±12 years. MVO was detected by CMR LGE imaging in 25 patients (63%). Table (1) shows baseline characteristics of patients stratified by the presence of MVO. There was no significant difference in demographics and cardiovascular risk factors between patients with and without MVO. Patients with MVO showed a higher peak troponin level versus those without MVO ( $p=0.001$ ) and a lower prevalence of RCA being the culprit artery (12% vs 47%,  $p=0.02$ ). LAD was the most common culprit vessel in the study cohort (63% of patients), followed by RCA (25%) and LCx (15%).

### *CMR Chamber volumes and function:*

As shown in Table (1), patients with MVO showed lower LV EF versus those without MVO (mean difference 11.3%,  $p=0.004$ ) with a trend towards higher BSA-indexed LV ESV (mean difference 12.5ml/m<sup>2</sup>;  $p=0.054$ ).

### *Tissue mapping characteristics:*

Native T1 mapping was performed in all patients, post-contrast T1 mapping in 37 patients,

and T2 mapping in 35 patients. On a segmental level, 551 segments (86%) out of 640 segments could be analyzed (i.e., had no artefacts) for native T1, 497 (84%) out of 592 for ECV, and 540 (96%) out of 560 for T2 values. Figs. (3,4) show segmental tissue mapping values for two example patients.

### *Hyperenhanced (acutely infarcted) myocardial regions versus remote regions:*

As shown in Table (2), hyperenhanced regions showed significantly higher native T1 (mean difference 60.8ms), ECV (median difference 11.5%), and T2 values (mean difference 5.5ms) compared to remote regions ( $p<0.001$  for all).

### *Hyperenhanced (acutely infarcted) myocardial segments versus remote ones:*

Table (3) shows tissue mapping characteristics of hyperenhanced segments versus remote ones. Hyperenhanced segments with and without MVO showed significantly higher native T1, ECV, and T2 values compared to remote ones ( $p<0.001$  for all). Versus hyperenhanced segments with no MVO, those with MVO showed significantly lower native T1 (mean difference 55.1ms), ECV (median difference 5%), and T2 values (mean difference 4ms;  $p<0.001$  for all).

### *Optimal cut-off tissue mapping values for detection of hyperenhanced (acutely infarcted) segments versus remote ones:*

ROC curve analysis of all analyzable myocardial segments yielded an optimal cut-off value of 1095ms for native T1, 36% for ECV, and 54ms for T2 to differentiate hyperenhanced segments versus remote ones. ROC curves for the three tissue mapping markers in all hyperenhanced segments and those with and without MVO versus remote segments are shown in Figs. (5,6,7). Diagnostic accuracies are shown in Table (4). While the specificities (72%-77%) and negative predictive values (NPV; 79%-86%) for all criteria were reasonable, sensitivities were low. ECV showed the highest sensitivity (73%), followed by T2 (63%), with native T1 having the worst (55%). Applying the same cut-off values to segments with no MVO yielded better diagnostic accuracy compared to those with MVO: Sensitivity using ECV criterion 87% for segments with no MVO versus 60% for MVO, T2 criterion 77% versus 51%, and native T1 69% versus 41%. All criteria yielded NPV above 90% for segments with no MVO.

Table (1): Baseline characteristics of the overall study population, stratified by microvascular obstruction (MVO).

Characteristic	Overall (n=40)	No MVO (n=15)	MVO (n=25)	<i>p</i> - value
<i>Demographics:</i>				
Age, years	53.4±12.1	50.3±8.9	55.2±13.5	0.17
Male sex	29 (72%)	12 (80%)	17 (68%)	0.49
<i>Risk factors:</i>				
Diabetes mellitus	12 (30%)	2 (13%)	10 (40%)	0.15
Hypertension	12 (30%)	6 (40%)	6 (24%)	0.31
Cigarette smoking	27 (68%)	11 (73%)	16 (64%)	0.73
Dyslipidemia	30 (75%)	12 (80%)	18 (72%)	0.71
Family history of CAD	11 (28%)	6 (40%)	5 (21%)	0.28
Known CAD	4 (10%)	1 (7%)	3 (12%)	0.999
<i>Index hospitalization:</i>				
Pain duration, minutes	408.8±305.4	396.0±235.6	416.4±345.0	0.83
Peak Troponin I, ng/ml	28.5±18.3	16.1±15.9	36.2±15.5	0.001
Duration of hospitalization, days	3.7±2.8	2.9±1.6	4.3±3.2	0.071
<i>Culprit vessel*:</i>				
LAD	25 (63%)	7 (47%)	18 (72%)	0.11
LCx	6 (15%)	2 (13%)	4 (16%)	0.999
RCA	10 (25%)	7 (47%)	3 (12%)	0.024
<i>CMR chamber volumes:</i>				
LV EDV, ml	145.2±34.9	139.2±40.4	148.8±31.5	0.44
LV EDVI, ml/m <sup>2</sup>	78.6±17.9	77.7±20.1	79.1±16.8	0.81
LV ESV, ml	82.2±31.6	69.2±29.6	90.1±30.7	0.041
LV ESVI, ml/m <sup>2</sup>	46.5±21.9	38.7±15.7	51.2±23.9	0.054
LV SV, ml	63.2±19.7	70.8±16.9	58.6±20.1	0.048
LV SVI, ml/m <sup>2</sup>	34.1±9.7	39.5±7.5	30.8±9.6	0.003
EF, %	44.5±13.3	51.5±10.1	40.2±13.4	0.004
<i>CMR tissue mapping values:</i>				
Hyperenhanced area native T1, ms	1,106.9±102.9	1,139.7±63.7	1,087.2±117.3	0.075
Remote area native T1, ms	1,046.1±58.3	1,034.9±36.5	1,052.7±68.0	0.29
Hyperenhanced area ECV, ms	44.1±17.6	52.5±24.4	39.0±9.2	0.066
Remote area ECV, ms	31.5±3.5	30.8±4.0	31.9±3.1	0.36
Hyperenhanced area T2, ms	56.8±5.7	59.1±5.1	55.2±5.6	0.041
Remote area T2, ms	51.3±4.5	52.1±3.4	50.8±5.1	0.35

Values are mean ± SD, median (IQR), or n (%).

CAD : Indicates coronary artery disease.

MVO : Microvascular obstruction.

LAD : Left anterior descending.

LCx : Left circumflex.

RCA : Right coronary artery.

LV : Left ventricle.

EDV(I) : End diastolic volume (indexed).

ESV(I) : End systolic volume (indexed).

SV(I) : Stroke volume (indexed).

EF : Ejection fraction.

ECV : Extracellular volume.

\*Categories do not sum up to 100% due to overlap.

Table (2): Tissue mapping in the hyperenhanced (acute MI) versus remote myocardial regions in the overall study cohort.

	Hyperenhanced region	Remote region	<i>p</i> -value*
Native T1, ms*	1106.9±102.9	1046.1±58.3	<0.001
ECV, %†	43.4 (36.5, 47.0)	31.9 (29.2, 33.1)	<0.001
T2, ms‡	56.8±5.7	51.3±4.5	<0.001

Values are mean ± SD or median (IQR).

ECV indicates extracellular volume.

\*Available for all study cohort (n=40)

†Available for 37 patients

‡Available for 35 patients

Table (3): Tissue mapping in the hyperenhanced (acutely infarcted) myocardial segments with and without MVO versus remote segments.

	Hyperenhanced segments, no MVO	Hyperenhanced segments, MVO	Remote segments	p-value
Native T1, ms*	1130.3±101.0†, ‡	1075.2±98.7 †	1043.8±96.7	<0.001
ECV, %§	44.0 (38.0, 53.0) †, ‡	39.0 (29.0, 47.0)†	29.0 (26.0, 36.0)	<0.001
T2, ms	58.6±6.8†, ‡	54.6±8.8†	51.5±6.4	<0.001

Values are mean ± SD or median (IQR).  
 ECV : Indicates Extracellular volume.  
 MVO: Microvascular obstruction.  
 \*Available for 551 segments.

†p-value <0.05 for post-hoc comparison against remote segments.  
 ‡p-value <0.05 for post-hoc comparison against hyperenhanced segments with MVO.  
 §Available for 497 segments.  
 ||Available for 540 segments.

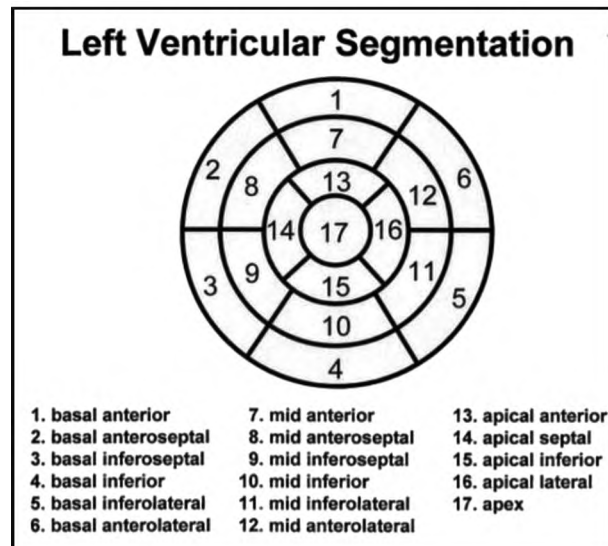
Table (4): Diagnostic accuracy of tissue mapping for detection of hyperenhanced (acutely infarcted) segments versus remote ones.

Criterion	Sensitivity	Specificity	PPV	NPV	Accuracy	AUC (95% CI)
<i>Native T1 &gt;1095 ms:</i>						
All HE segments	55 %	77%	52%	79%	70%	0.68 (0.67-0.70)
HE segments, no MVO	69%	77%	40%	92%	76%	0.77 (0.75-0.79)
HE segments, MVO	41%	77%	29%	85%	71%	0.61 (0.58-0.63)
<i>ECV&gt;36%:</i>						
All HE segments	73 %	74%	55%	86%	73 %	0.78 (0.76-0.79)
HE segments, no MVO	87 %	74%	42%	96%	76%	0.86 (0.84-0.87)
HE segments, MVO	60%	74%	34%	89%	71%	0.70 (0.67-0.72)
<i>T2&gt;54 ms:</i>						
All HE segments	63 %	72%	53%	79%	69%	0.71 (0.69-0.72)
HE segments, no MVO	77%	72%	39%	93%	73 %	0.79 (0.78-0.81)
HE segments, MVO	51%	72%	32%	85%	67 %	0.63 (0.61-0.65)

PPV: Indicates positive predictive value.  
 NPV: Negative predictive value.  
 AUC, ROC: Area under the curve.  
 CI: Confidence interval.

ECV : Extracellular volume.  
 MVO : Microvascular obstruction.  
 HE : Hyperenhanced.

Fig. (1): Display, on a circumferential polar plot, of the myocardial segments according to AHA 17-segment model and the recommended nomenclature for tomographic imaging of the heart.



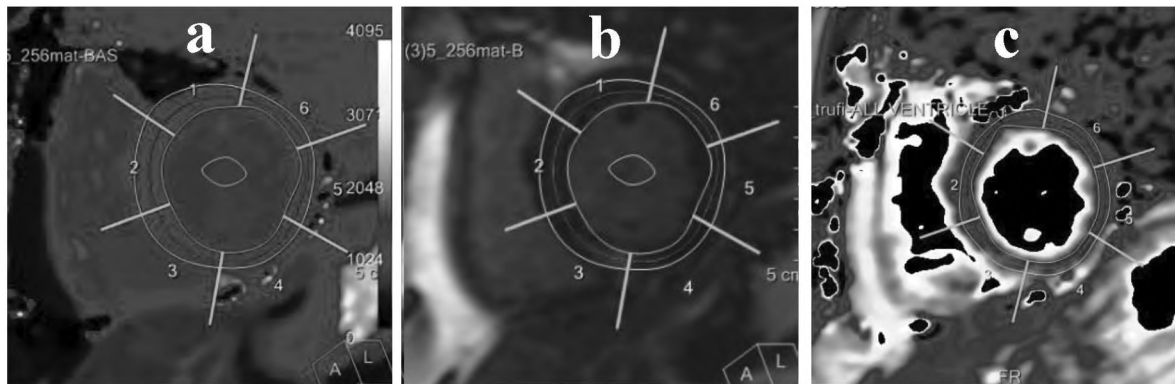


Fig. (2): Short axis basal LV slice with pre- (A) and post-contrast (B) T1 mapping and T2 mapping (C) images divided into 6 segments, with blood ROI in T1 map images to calculate ECV values.

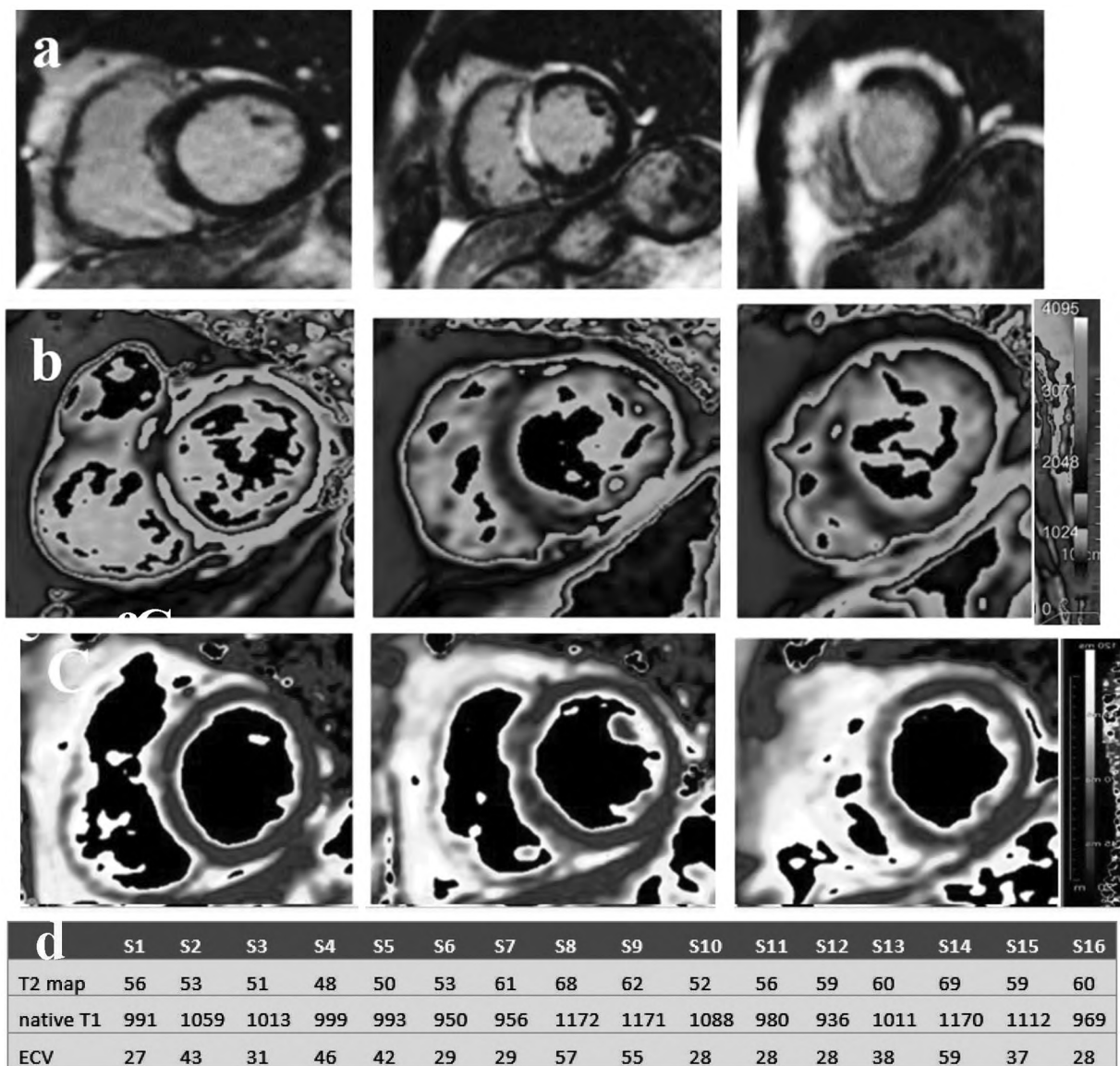


Fig. (3): Example patient 1: 53-year old male patient. (a, b, c) Short axis images at basal, mid-ventricular, and apical levels. (A) LGE images show transmural enhancement at the midventricular septal wall and subendocardial enhancement at the apical septal and inferior walls. (B) native T1 images show corresponding signal change at mid-ventricular septal wall as well as apical septal and inferior walls. (C) T2 map images show similar corresponding signal change at midventricular septal wall as well as apical septal & inferior walls. (D) quantitative assessment of the 16 myocardial segments showing values of T2, native T1, and ECV.

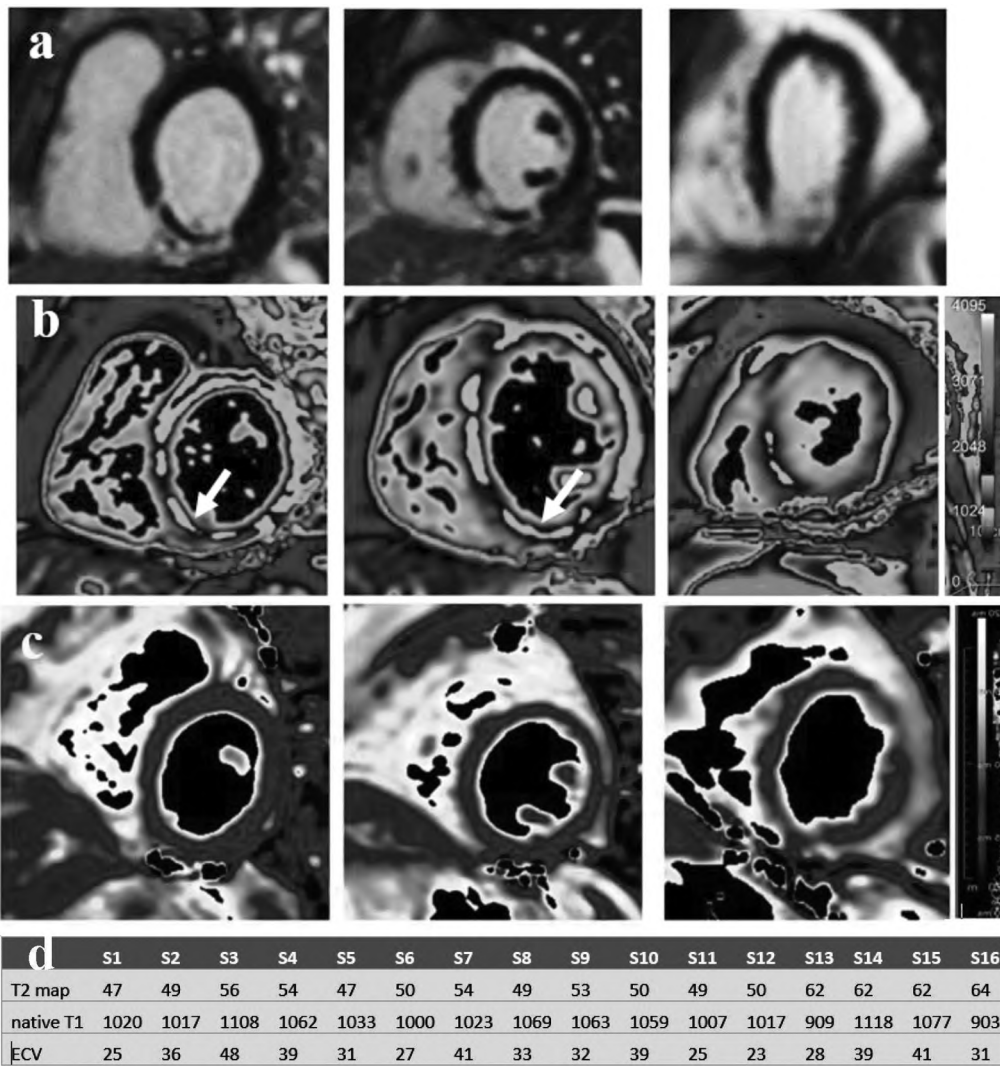


Fig. (4): Example patient 2: 49-year old male patient. (A, B, C) Short axis images at basal, mid-ventricular, and apical levels. (A) LGE images show transmurular enhancement at the basal and mid-ventricular infero-septum and basal to apical inferior wall with MVO noted at the basal and mid-ventricular levels. (B) native T1 images show corresponding signal change with a central pseudo-normalized area corresponding to MVO “arrows”. (C) T2 map images show no appreciable signal change at basal and midventricular levels (levels of MVO) with evident signal change at apical level. (D) Quantitative assessment of the 16 myocardial segments showing values of T2, native T1, and ECV. The quantitative assessment highlights the effect of MVO on pseudo normalization of native T1, T2, and ECV values at basal and mid-ventricular levels.

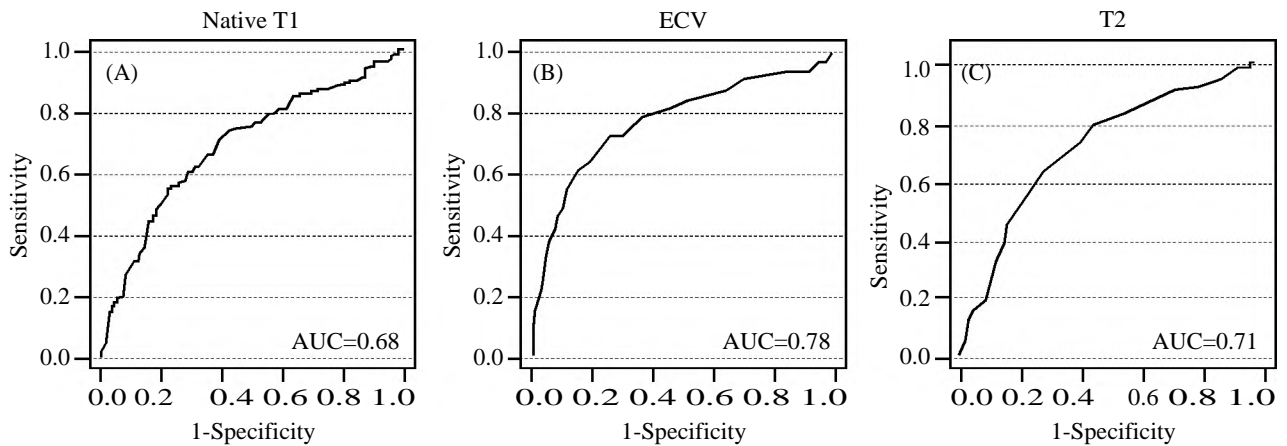


Fig. (5): ROC curves for detection of acutely infarcted segments using native T1 (A), ECV (B), and T2 values (C) in all hyperenhanced segments versus remote segments. The three graphs were not grouped into one due to different number of segments.

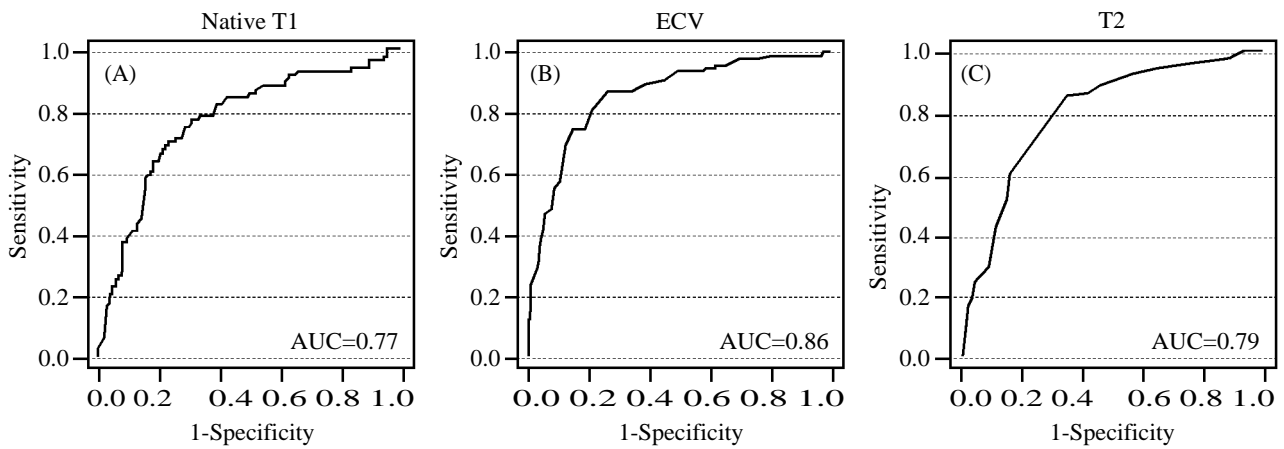


Fig. (6): ROC curves for detection of acutely infarcted segments using native T1 (A), ECV (B), and T2 values (C) in hyperenhanced segments without MVO versus remote segments. The three graphs were not grouped into one due to different number of segments.

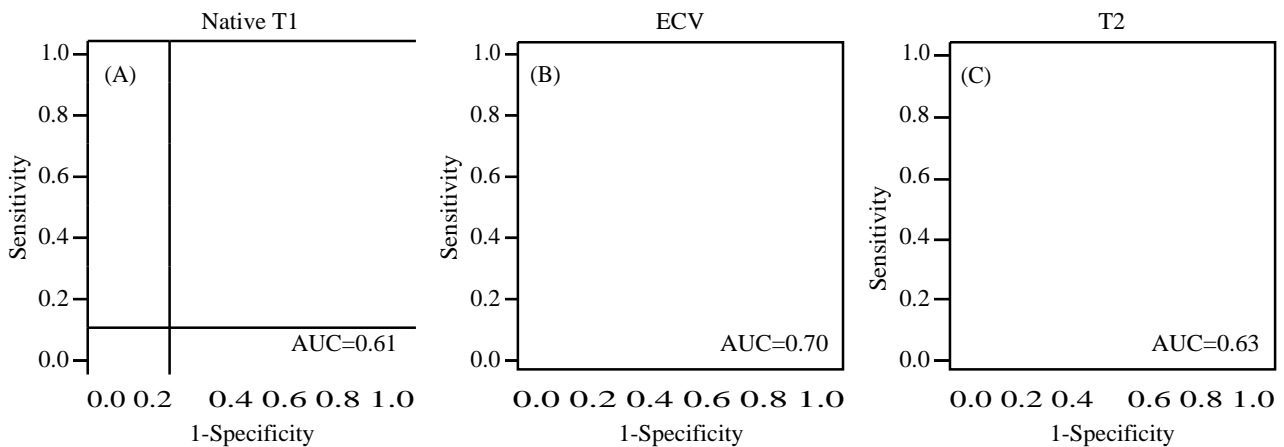


Fig. (7): ROC curves for detection of acutely infarcted segments using native T1 (A), ECV (B), and T2 values (C) in hyperenhanced segments with MVO versus remote segments. The three graphs were not grouped into one due to different number of segments.

### Discussion

Cardiac magnetic resonance (CMR) imaging offers the unique opportunity to assess the myocardium non-invasively [22]. Our study highlights the potential of tissue mapping to detect acute myocardial injury as evidenced by significant differences of tissue mapping values between hyperenhanced (infarcted) and remote regions / segments. Our suggested optimal cut-off values for native T1 (1095 ms) and T2 (54ms) to differentiate hyperenhanced segments versus remote ones showed reasonable specificities (77% and 72%) and NPVs (79% for each); however, sensitivities were generally low (55% and 63%). Applying the same cut-off values to segments with no MVO yielded better diagnostic accuracy compared to those with MVO. These results highlight the pseudo-normalization effect of MVO on tissue mapping readings.

Our finding of significant differences in tissue mapping values between hyperenhanced and remote regions/segments is in line with previous studies [11-15]. The study conducted by Dall'Armellina et al., [12] using a 3-T scanner showed statistically significant difference of native T1 values between the remote & hyperenhanced segments. They showed mean native T1 value of the hyperenhanced segments of about  $1257 \pm 97$ ms compared to  $1196 \pm 56$ ms in the remote segments with  $p$ -value  $< 0.01$ . E Tahir et al. [11] stated that native T1 and T2 may provide a reliable noninvasive means of recognizing AMI with mean T1 & T2 values of the remote myocardium are  $1036 \pm 42$ ms &  $55 \pm 3$ ms respectively in their study using a 1.5-T scanner. It's to be noted that the mean native T1 values in our study approaches that of the study conducted E Tahir et al. & both are less than that of the study conducted by Dall'Armellina et al. A finding that can be

attributed to the difference in the magnetic field strength.

The studies reporting optimal cut-offs to differentiate hyperenhanced and remote segments conducted by Bulluck et al., Cui et al. & Kali et al. [13-15] showed superior diagnostic accuracy compared to ours (sensitivity 76-94%, specificity 74-94%, and AUC 0.86-0.96). Two important causes for this discrepancy are an animal study cohort in the studies by Kali et al. and Cui et al. and scanning at 3-T in the studies by Kali et al. (in addition to a subset performed at 1.5-T) and Bulluck et al. A higher magnetic field is associated with better signal to noise ratio, potentially leading to superior diagnostic performance with 3-T versus 1.5-T scanner. The latter is confirmed by the higher diagnostic accuracy of cut-off values for the subset of animals scanned at 3-T versus those scanned at 1.5-T in the study by Kali et al. (respective sensitivity, specificity, and AUC 94%, 94%, and 0.96 versus 84%, 74%, and 0.86 for 3-T versus 1.5T). Finally, the study by Bulluck et al. involved only 18 human patients - a sample size that might be too small to be adequately representative of the true population of acute MI.

To our knowledge, this is the second study to report on the diagnostic accuracy of both native T1 and T2 values to detect acutely infarcted myocardial segments in a reasonably sized patient cohort at 1.5-T. This has potential implications in the diagnostic pathways for patients with suspected acute MI, especially those with CKD. Future developments in tissue mapping sequences might improve their diagnostic accuracy.

We acknowledge important limitations that the study was conducted at a tertiary referral center with consequent possible referral bias. Our gold standard was LGE imaging that may not be the 'true' ground truth as opposed to histopathological examination, especially with small or very early infarcts.

#### Conclusion:

Native (non-contrast) tissue mapping has the potential to detect acutely infarcted myocardial segments with implications for the diagnostic pathways in patients with chronic kidney disease. However, the pseudo normalization effect of MVO lowers the diagnostic accuracy of this modality, with the need to improve currently used imaging sequences to permit their routine application in clinical practice.

#### References

- 1- Global health estimates: Leading causes of death 2020: Deaths by Cause, Age, Sex, by Country and by Region, 2000-2019. Geneva, World Health Organization. <https://www.who.int/data/gho/data/themes/mortality-and-global-health-estimates/ghes-leading-causes-of-death>, 2020.
- 2- KNUUTI J., WIJNS W., SARASTE A., et al.: 2019 ESC Guidelines for the diagnosis and management of chronic coronary syndromes. *Eur. Heart J.* <https://doi.org/10.1093/eurheartj/ehz425>, 2019.
- 3- BARITUSSIO A., SCATTEIA A., BUCCIARELLI-DUCCI C.: Role of cardiovascular magnetic resonance in acute and chronic ischemic heart disease. *Int. J. Cardiovasc. Imaging*, 34: 67-80. <https://doi.org/10.1007/s10554-017-1116-0>, 2018.
- 4- CORNELISSEN V.: 2020 ESC Guidelines for the management of acute coronary syndromes in patients presenting without persistent ST-segment elevation. *Eur. Heart J* 1-79. <https://doi.org/10.1093/eurheartj/ehaa575>, 2020.
- 5- KIM R.J., FIENO D.S., PARRISH T.B., et al.: Relationship of MRI delayed contrast enhancement to irreversible injury, infarct age, and contractile function. *Circulation*, 100: 1992-2002. <https://doi.org/10.1161/01.CIR.100.19.1992>, 1999.
- 6- PATERSON D.I., WHITE J.A., BUTLER C.R., et al.: 2021 Update on Safety of Magnetic Resonance Imaging: Joint Statement From Canadian Cardiovascular Society/Canadian Society for Cardiovascular Magnetic Resonance/Canadian Heart Rhythm Society. *Can J Cardiol* 37:835-847. <https://doi.org/10.1016/j.cjca.2021.02.012>, 2021.
- 7- FOX C.S., MUNTNER P., CHEN A.Y., et al.: Use of evidence-based therapies in short-term outcomes of ST-segment elevation myocardial infarction and non-ST-segment elevation myocardial infarction in patients with chronic kidney disease: A report from the National Cardiovascular Data Acute Coronary. *Circulation*, 121: 357-365. <https://doi.org/10.1161/CIRCULATIONAHA.109.865352>, 2010.
- 8- YANG H., LIU J., LUO H., et al.: Improving the diagnostic accuracy of acute myocardial infarction with the use of high-sensitive cardiac troponin T in different chronic kidney disease stages. *Sci. Rep.* 7: 1-7. <https://doi.org/10.1038/srep41350>, 2017.
- 9- PEREA R.J., ORTIZ-PEREZ J.T., SOLE M., et al.: T1 mapping: characterisation of myocardial interstitial space. *Insights Imaging* 6:189-202. <https://doi.org/10.1007/s13244-014-0366-9>, 2015.
- 10- KIM P.K., HONG Y.J., IM D.J., et al.: Myocardial T1 and T2 mapping: Techniques and clinical applications. *Korean J Radiol* 18: 113-131. <https://doi.org/10.3348/kjr.2017.18.1.113>, 2017.
- 11- TAHIR E., SINN M., BOHNEN S., et al.: Acute versus chronic myocardial infarction: Diagnostic accuracy of quantitative native T1 and T2 mapping versus assessment of edema on standard T2-weighted cardiovascular MR images for differentiation. *Radiology*, 285: 83-91. <https://doi.org/10.1148/radiol.2017162338>, 2017.
- 12- Dall'Armellina E., Piechnik S.K., Ferreira V.M., et al.: Cardiovascular magnetic resonance by non contrast T1-

- mapping allows assessment of severity of injury in acute myocardial infarction. *J. Cardiovasc. Magn Reson*, 14: 1-13. <https://doi.org/10.1186/1532-429X-14-15>, 2012.
- 13- BULLUCK H., WHITE S.K., ROSMINI S., et al.: T1 mapping and T2 mapping at 3T for quantifying the area-at-risk in reperfused STEMI patients. *J. Cardiovasc. Magn Reson*, 17: 1-10. <https://doi.org/10.1186/s12968-015-0173-6>, 2015.
- 14- CUI C., WANG S., LU M., et al.: Detection of recent myocardial infarction using native T1 mapping in a swine model: A validation study. *Sci. Rep.*, 8: 1-10. <https://doi.org/10.1038/s41598-018-25693-1>, 2018.
- 15- KALI A., COKIC I., TANG R.L.Q., et al.: Determination of location, size, and transmural extent of chronic myocardial infarction without exogenous contrast media by using cardiac magnetic resonance imaging at 3 T. *Circ Cardiovasc Imaging*, 7: 471-481. <https://doi.org/10.1161/CIRCIMAGING.113.001541>, 2014.
- 16- THYGESEN K., ALPERT J.S., JAFFE A.S., et al.: Fourth universal definition of myocardial infarction (2018). *Eur Heart J* 40:237-269. <https://doi.org/10.1093/eurheartj/ehy462>, 2019.
- 17- SCHULZ-MENGER J., BLUEMKE D.A., BREMERICH J., et al.: Standardized image interpretation and post processing in cardiovascular magnetic resonance: Society for Cardiovascular Magnetic Resonance (SCMR) board of trustees task force on standardized post processing. *J. Cardiovasc. Magn Reson*, 15: 1-19. <https://doi.org/10.1186/1532-429X-15-35>, 2013.
- 18- BRONCANO J., BHALLA S., CARO P., et al.: Cardiac MRI in Patients with Acute Chest Pain. *RadioGraphics*, 41: 8-31. <https://doi.org/10.1148/rg.2021200084>, 2021.
- 19- CERQUEIRA M.D., WEISSMAN N.J., DILSIZIAN V., et al.: Standardized myocardial segmentation and nomenclature for tomographic imaging of the heart: a statement for healthcare professionals from the Cardiac Imaging Committee of the Council on Clinical Cardiology of the American Heart Association. *Circulation*, 105: 539-542. <https://doi.org/10.1161/hc0402.102975>, 2002.
- 20- HAAF P., GARG P., MESSROGHLI D.R., et al.: Cardiac T1 mapping and extracellular volume (ECV) in clinical practice: A comprehensive review. *J. Cardiovasc. Magn Reson* 18:1-12. <https://doi.org/10.1186/s12968-016-0308-4>, 2017.
- 21- YODEN W.J.: Index for rating diagnostic tests. *Cancer* 3:32-35. [https://doi.org/10.1002/1097-0142\(1950\)3:1<32::AID-CNCR2820030106>3.0.CO;2-3](https://doi.org/10.1002/1097-0142(1950)3:1<32::AID-CNCR2820030106>3.0.CO;2-3), 1950.
- 22- DOESCH C.: Diagnosis and management of ischemic cardiomyopathy: Role of cardiovascular magnetic resonance imaging. *World J. Cardiol.*, 6: 1166. <https://doi.org/10.4330/wjc.v6.i11.1166>, 2014.

## الدقة التشخيصية لرسم خرائط الأنسجة بتصوير الرنين المغناطيسي في احتشاء عضلة القلب الحاد

مرض الشريان التاجي هو السبب الأكثر شيوعاً للوفاة في جميع أنحاء العالم. يمكن أن يكون الرنين المغناطيسي للقلب مفيداً في الحالات المشتبه بها، في حين أن تصوير تعزيز الصبغة المتأخر هو المعيار الذهبي الحالي في الجسم الحي للكشف عن احتشاء عضلة القلب الحاد، فإن استخدام الصبغة يمكن أن يكون مشكلة في المرضى الذين يعانون من اختلال وظائف الكلى. كنا نهدف إلى استكشاف الدقة التشخيصية لرسم خرائط الأنسجة لإكتشاف احتشاء عضلة القلب الحاد، مقارنة بصور تعزيز الصبغة المتأخر.